

## Anti-corrosion properties of niaouli essential oil for tinfoil in 3 %NaCl medium

R. Nabah<sup>1,2</sup>, H. Lgaz<sup>1</sup>, H. Zarrok<sup>1</sup>, M. Larouj<sup>1</sup>, F. Benhiba<sup>1</sup>, K. Ourrak<sup>3</sup>,  
M. Cherkaoui<sup>2</sup>, A. Zarrouk<sup>4</sup>, R. Tourir<sup>5,6</sup>, H. Oudda<sup>1\*</sup>

<sup>1</sup> Laboratory of Separation Processes, Faculty of Science, University IbnTofail PO Box 242, Kenitra, Morocco.

<sup>2</sup> Laboratory of Matériaux, Electrochimie and Environnement, Faculty of Science, University IbnTofail PO Box 242 Kenitra, Morocco.

<sup>3</sup> Laboratory of Chimie Physique, Faculty of Sciences, University Moulay Ismail, Meknès, Morocco.

<sup>4</sup> LC2AME, Faculty of Science, First Mohammed University, PO Box 717, 60 000 Oujda, Morocco.

<sup>5</sup> Laboratoire d'Ingénierie des Matériaux et d'Environnement : Modélisation et Application, Faculté des Sciences, Université Ibn Tofail, BP 133, Kénitra 14 000, Morocco.

<sup>6</sup> Centre Régional des Métiers de l'Education et de la Formation (CRMEF), Avenue Allal Al Fassi, Madinat Al Irfane BP 6210 Rabat, Morocco.

Received 14 Feb 2017,  
Revised 19 Jun2017,  
Accepted 21 Jun 2017

### Keywords

- ✓ Tinplate;
- ✓ NaCl;
- ✓ Corrosion inhibition;
- ✓ Niaouli Essential Oil;
- ✓ Electrochemical techniques;

[ouddahassan@gmail.com](mailto:ouddahassan@gmail.com)

### Abstract

Niaouli Essential Oil (NEO) was analyzed by GC and GC/MS and its mainly compound is the Eucalyptol (60.01%). The corrosion inhibition of Niaouli Essential Oil (NEO) on tinfoil has been studied in 3% NaCl at pH = 2 by Tafel polarization and electrochemical impedance spectroscopy (EIS) techniques. The results showed that the inhibition efficiency of NEO increases with concentration and decreases with temperature. It was found that NEO behaves as a cathodic inhibitor at the concentration range 0.1-0.4 g L<sup>-1</sup> and a mixed type inhibitor at 0.5 g L<sup>-1</sup>. EIS showed that the inhibitor addition decreases the double-layer capacitance and increases the polarization resistance. The adsorption process of NEO obeyed the Langmuir isotherm.

## 1. Introduction

Tinplate is widely used in industry. This is due to several factors including good resistance to corrosion and its low toxicity. The layer of tin deposited on the material surface consists essentially of a thin sheet of carbon rolled steel and tin plated by a layer of pure tin on both sides. Between the layer of pure tin and steel, it forms an intermediate layer composed of a solid solution Fe-Sn [1]. When this layer is not compact and continuous, the steel is exposed through the pores to aggressive food compounds or food additives and corrosion is accelerated. The thickness requirements of the tin coating depend on the products type that can will contain. During food and beverage packaging in tinplate, the dissolution of tin into food content may occur [2-4].

To avoid tin and iron contamination of the canned food, lacquers [5-8] or different kinds of corrosion inhibitors [9,10] can be used to protect the metallic substrate.

While their application is not always simple and cost-effective. An inhibitor can be chosen from compounds that have hetero atoms in their aromatic ring system or synthesized from cheap raw materials [11-21]. However, the problem of finding an inhibitor that has little or no impact on the environment has attracted numerous researches in recent times [22]. Over the past couple of decades, studies have focused on the application of non-toxic inhibitors called green or eco-friendly environmental inhibitors. Among the various essential oils of natural products, such as the Jojoba oil [23], Rosemary oil [24,25], Artemisia oil [26,27], Argan oil [28] and eucalyptus oil [29,30] have been evaluated as the good inhibitors against corrosion.

In the present work, the chemical composition of Niaouli Essential Oil (NEO) is established using GC and GC-MS. Then, its inhibition performance for tinplate in 3% NaCl was evaluated by electrochemical techniques.

## 2. Experimental details

### 2.1. Characterization and chemical composition of essential oils

Techniques in chromatography (GC/MS, GC-FTIR, HPLC-DAD) are available for the molecular analysis of organic compounds. The chemical components of Niaouli Essential Oil was determined by spectral analysis of gas chromatography and gas chromatography coupled to mass spectrometry (GC-MS), which identified six major components. GC analyses were performed using a Perkin-Elmer Autosystem GC apparatus (Waltham, MA, USA) equipped with a single injector and two flame ionization detectors (FID). The apparatus was used for simultaneous sampling with two fused-silica capillary columns (60 m long with i.d. 0.22 mm, film thickness 0.25  $\mu\text{m}$ ) with different stationary phases: Rtx-1 (polydimethylsiloxane) and Rtx-Wax (polyethylene glycol). The temperature program was for 333-503K at 275K/min and then held at isothermal 503K (30 min). The carrier gas was helium (1 mL/min). Injector and detector temperatures were held at 553K. Split injection was conducted with a ratio split of 1:80. Electron ionization mass spectra were acquired with a mass range of 35-350 Da. The injected volume of oil was 0.1  $\mu\text{L}$ . For gas chromatography-mass spectrometry, the oils obtained were investigated using a Perkin-Elmer Turbo Mass Quadrupole Detector, directly coupled to a Perkin-Elmer Auto system XL equipped with two fused-silica capillary columns (60 m long with i.d. 0.22 mm, film thickness 0.25  $\mu\text{m}$ ), with Rtx-1 (polydimethylsiloxane) and Rtx-Wax (polyethylene glycol). Other GC conditions were the same as described above. Ion source temperature was 423 K and energy ionization 70 eV. Electron ionization mass spectra were acquired with a mass range of 35-350 Da.

The injected volume of oil was 0.1  $\mu\text{L}$ . Identification of the components was based (1) on the comparison of their GC retention indices (RI) on non-polar and polar columns, determined relative to the retention time of a series of n-alkanes with linear interpolation, with those of authentic compounds or literature data [31], and (2) on computer matching with commercial mass spectral libraries [31,32] and comparison of spectra with those in our personal library. Relative amounts of individual components were calculated on the basis of their GC peak areas on the two capillary Rtx-1 and Rtx-Wax columns, without FID response factor correction.

### 2.2. Materials and solutions

The employed material in this study is the tinplate (Low carbon content, less than 0.08%) with a thick of 0.2 mm covered with a thin layer of 1  $\mu\text{m}$ . It has been selected based on its diverse uses in packing food and beverage cans. For electrochemical tests, the tinplate samples are used as a working electrode that is rinsed with acetone and with distilled water. The experiments were carried out in 3% NaCl at pH = 2 solution in the absence and presence of inhibitor at different concentrations range of 0.1-0.5g/L. All aqueous solutions were prepared from distilled water and analytical grade chemicals.

### 2.3. Electrochemical measurements

The electrochemical measurements were carried out using Volta lab (Tacussel- Radiometer PGZ 100) potentiostat and controlled by Tacussel corrosion analysis software model (Voltmaster 4) at under static condition. A saturated calomel electrode (SCE) and platinum electrode were used as reference and auxiliary electrodes, respectively. All potentials were referred to the SCE. The working electrode was immersed in test solution for 30 min to establish steady state open circuit potential (E<sub>ocp</sub>). After measuring the E<sub>ocp</sub>, the electrochemical measurements were performed. All electrochemical tests have been performed in aerated solutions at 298 K. The EIS experiments were conducted in the frequency range with high limit of 100 kHz and different low limit 0.1 Hz at open circuit potential, with 10 points per decade, at the rest potential after 30 min of acid immersion, by applying 10 mV ac voltage peak-to-peak. The best semicircle can be fit through the data points in the Nyquist plot using a non-linear least square fit so as to give the intersections with the x-axis.

The inhibition efficiency of the inhibitor was calculated from the polarization resistance values using the following equation:

$$\eta_z \% = \frac{R_p^i - R_p^\circ}{R_p^i} \times 100 \quad (1)$$

Where,  $R_p^\circ$  and  $R_p^i$  are the polarization resistance in the absence and the presence of inhibitor, respectively.

After ac impedance test, the potentiodynamic polarization measurements of tinplate substrate in inhibited and uninhibited solution were scanned from cathodic to the anodic direction, with a scan rate of 1 mV s<sup>-1</sup>.

The potentiodynamic data were analyzed using the polarization VoltMaster 4 software. The linear Tafel segments of anodic and cathodic curves were extrapolated to corrosion potential to obtain corrosion current densities ( $i_{\text{corr}}$ ). The inhibition efficiency was evaluated using the following relationship:

$$\eta_{\text{Tafel}}(\%) = \frac{i_{\text{corr}} - i_{\text{corr}(i)}}{i_{\text{corr}}} \times 100 \quad (2)$$

where  $i_{\text{corr}}$  and  $i_{\text{corr}(i)}$  are the corrosion current densities for tinplate electrode in the uninhibited and inhibited solutions, respectively.

### 3. Results and Discussion

#### 3.1. Niaouli essential oil (NEO) analysis

The analysis of essential oil from Niaouli essential oil was carried out by GC and GC/MS. Its chemical composition was characterized by 14 compounds, which accounted for 95.58% of the total oil, and summarized in Table 1. It is noted that the major components were  $\alpha$ -Pinene (6.24%), D-Limonene (6.50%), Eucalyptol (60.01%),  $\alpha$ -Terpineol (6.49%) and Epiglobulol (6.26%).

**Table 1:** Chemical composition of Niaouli essential oil.

Compounds	Percentage (%)
$\alpha$ -Pinene	6.24
$\beta$ -Pinene	1.67
$\beta$ -Myrcene	0.63
D-Limonene	6.50
p-Mentha-1,3,8-triene	0.94
Eucalyptol	60.01
4-Thujanol	1.02
1-Terpinen-4-ol	0.56
$\alpha$ -Terpineol	6.49
p-Menth-1-en-8-ol, acetate	0.96
Caryophyllene	1.89
Varidiflorene	1.47
Epiglobulol	6.26
Ledol	0.94

#### 3.2. Potentiodynamic polarization curves

The corrosion of tinplate electrode in 3% NaCl (pH = 2) solutions containing various concentrations of NEO was studied by potentiodynamic polarization. Fig. 1 shows the polarization curves, and their electrochemical parameters such as corrosion potential ( $E_{\text{corr}}$ ), corrosion current density ( $i_{\text{corr}}$ ), cathodic Tafel slopes ( $\beta_c$ ), and inhibition efficiencies  $\eta_{\text{Tafel}}$  (%) are listed in Table 2.

It can be observed from the potentiodynamic polarization curves that the presence of Niaouli essential oil causes a decrease in both the anodic and cathodic current densities. These results could be explained by the adsorption of organic compounds that are present in the Niaouli essential oil at the active sites of the metallic surface. It can be also explained by that the NEO molecules retards the metallic dissolution and hydrogen evolution and consequently, slows the corrosion process.

Table 1 revealed that the corrosion current densities ( $i_{\text{corr}}$ ) decrease with NEO concentrations to reach a minimum at 0.5g/L. This decrease suggested that the inhibitor retards the corrosion reaction by the formation of protective film on the tinplate surface, which created a barrier between metal and corrosive medium. It is noted at this concentration that both  $\beta_a$  and  $\beta_c$  were affected by inhibitor addition with a change in the corrosion potential. This was indicative of the mixed-mode inhibitive nature of the inhibitor at 0.5 g/L. For the other concentration (from 0.1 g/L to 0.4 g/L) the inhibitor acts as cathodic inhibitor

#### 3.3. Electrochemical impedance spectroscopy

The method is widely used for investigation of the corrosion inhibition process. The technique is based on measurement of the impedance of the double layer at the metal/solution interface [33]. The metal-solution interface behaves as a capacitor with the metal surface acting as one plate. The other plate is built of solvated ions of the electrolyte and the closest distance of approach of the centers of these ions is called outer Helmholtz plane (OHP). In addition, ions can be specifically adsorbed and their centres are then located at the inner Helmholtz plane. Outside the inner, or compact double layer, ions are organised in a diffuse layer which acts as a capacitor in series with that of the Helmholtz layer [34].

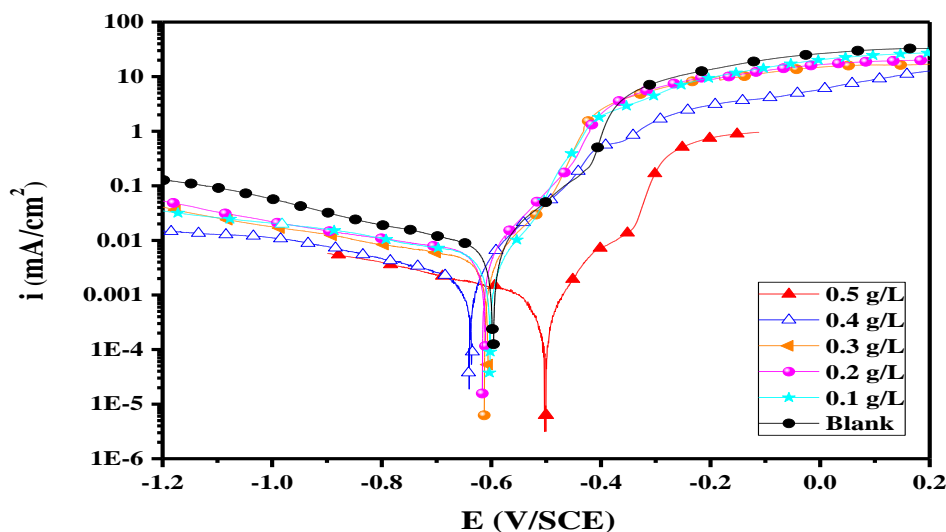


**Fig. 1:** Potentiodynamic polarisation curves of tinplate in 3% NaCl, for various concentrations of NEO at 298 K

**Table 2:** Electrochemical parameters for tinplate in 3% NaCl at pH= 2 at different concentration of NEO at 298K

C(g/L)	- E <sub>corr</sub> (mV /SCE)	i <sub>corr</sub> ( $\mu$ A/cm <sup>2</sup> )	$\beta_a$ (mV/dec)	$-\beta_c$ (mV/dec)	$\eta_{Tafel}$ (%)
00	585	7700	12 .9	271.3	
0.1	579	6200	32 .5	192.0	19
0.2	602	5200	38 .1	119.6	32
0.3	601	4100	46.4	117.3	46
0.4	627	2100	27.0	111.4	72
0.5	489	0910	25.0	102.7	88

In general, for a corrosion system, the equivalent circuit is given as in Fig. 2. The impedance response of a corrosion system is resembled to a parallel combination of a capacitor,  $C_{dl}$ , and a resistor,  $R_t$ , both in series with another resistor  $R_s$ . The impedance of the circuit given in Fig. 2 can be calculated as follows:

$$Z = R_s + \frac{R_t}{1 + j\omega C_{dl} R_t} \quad (3)$$

where  $R_s$  is the solution resistance,  $R_t$  the charge transfer resistance,  $j$  is the imaginary unit ( $\sqrt{-1}$ ),  $\omega$  the angular frequency ( $\omega=2\pi f$ ) and  $C_{dl}$  is the double layer capacitance [33].

The corrosion of tinplate in 3% NaCl solution in the absence and presence of NEO at different concentrations was also investigated by electrochemical impedance spectroscopy (EIS) after 0.5 h of immersion. The obtained results at the open circuit potential are shown in Fig. 3 and the electrochemical data are presented in Table 3.

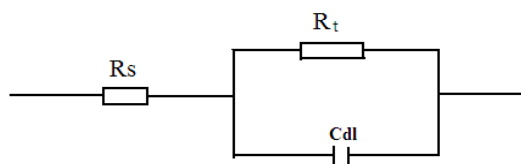


**Fig. 2:** Generally accepted equivalent circuit for metal/solution interface.

It is seen that these plots were composed from one single semicircle indicating the presence of single charge transfer process during dissolution which is unaffected by the presence of inhibitor molecules [35]. These plots are not semicircles as expected from the theory of AC impedance technique, they are suppressed semicircles. This situation can be explained as follows: the electronic equivalent circuits which are especially designed to fit the equivalent circuit models give semicircle Nyquist plots. Real condensers are used in specially prepared dummy cells and the charge distribution controlled by electrons in these cells which consist two metallic plates.

In a corrosion system, formation of a double layer at the metal/solution interface occurs. For corroded metals the double layer on the metal/solution interface does not behave as a real condenser. On the metal side of the double layer, the charge distribution is controlled by ions. Since ions are much larger than the electrons, the equivalent ions to the charge on the metal will occupy quite a large volume on the solution side of the double layer [36,37].

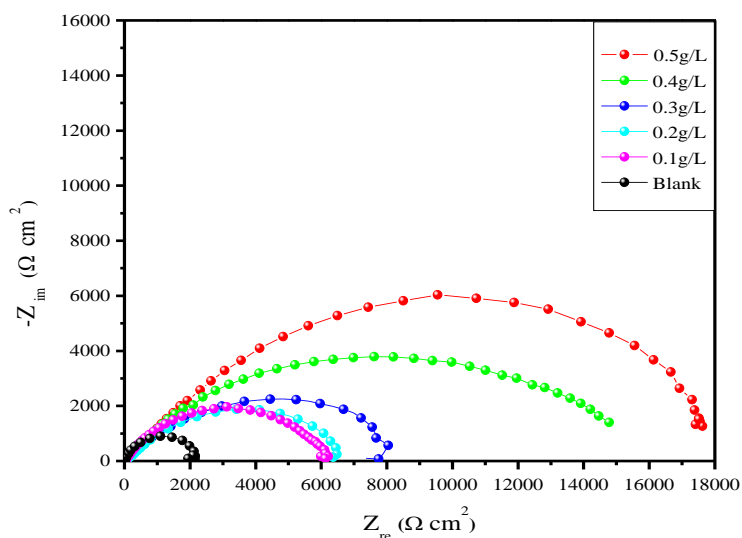


**Fig. 3:** Nyquist diagrams for tinplate electrode in 3% NaCl at pH = 2 at various concentrations of NEO at 298K.

It is apparent from Table 3, that the polarization resistance ( $R_p$ ) value of tinplate in 3 % NaCl (pH = 2) solution increases from  $2220 \Omega \text{ cm}^2$  for the blank solution to  $18305 \Omega \text{ cm}^2$  in the presence of 0.5 g/L of NEO. So, the difference in real impedance at lower and higher frequencies is considered as charge transfer resistance ( $R_t$ ). The resistance between the metal and OHP must be equal to the  $R_t$  but in the present paper  $R_p$  was used instead of  $R_t$  which has been discussed elsewhere [33]. In addition, it is clear that the capacitance of the double-layer value decreases with NEO concentration. This change was caused by the gradual replacement of water molecules by the chloride anion and/or by the organic molecules adsorption on metallic surface, decreasing the extent of dissolution reaction [38].

**Table 3:** EIS parameters for tinplate corrosion in 3% NaCl (pH = 2) at various concentrations of NEO at 298 K

C(g/L)	$R_s(\Omega \text{ cm}^2)$	$R_p(\Omega \text{ cm}^2)$	$C_{dl}(\mu\text{F}/\text{cm}^2)$	$\eta_z(\%)$
Blank	0.80	2220	10.8	
0.1	18.27	6170	7.42	64.1
0.2	20.00	6427	4.40	65.4
0.3	20.10	7990	4.16	72.2
0.4	23.34	15568	2.82	85.7
0.5	39.10	18305	1.87	88.0

### 3.4. Effect of temperature

The composition of the medium and its temperature are essential parameters affecting the corrosion phenomenon. The influence of temperature on the inhibition efficiency of NEO was conducted at 0.5 g/L concentration in the temperature range of 298-328 K. The representative curves in the absence and presence of 0.5g/L NEO are shown in Figs. 4 and 5, respectively, and their electrochemical parameters reported in Table 4.

It is noted that the inhibition efficiencies decrease with increasing the solution temperature from 298 K to 328 K. This behavior can be interpreted on the basis that the increases in temperature results in desorption of the inhibitor molecules from the tinplate surface. Table 4 shows that the corrosion rate increases with temperature both in uninhibited and inhibited solutions. It is remarked that the corrosion rate increases more rapidly with temperature in the uninhibited solution. These results confirm that NEO acts as an efficient inhibitor for tinplate in 3 % NaCl in the studied temperature range.

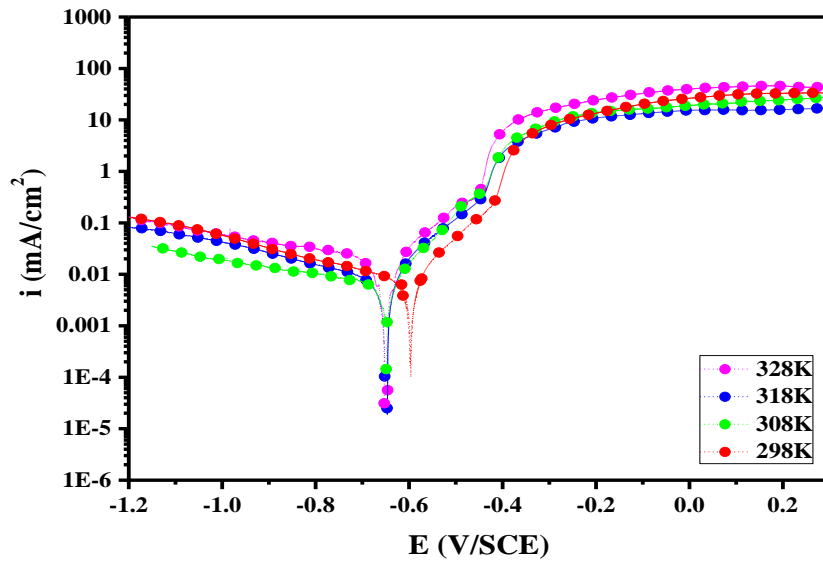


**Fig. 4:** Potentiodynamic polarization curves of tinplate in 3% NaCl (pH = 2) without NEO at various temperatures

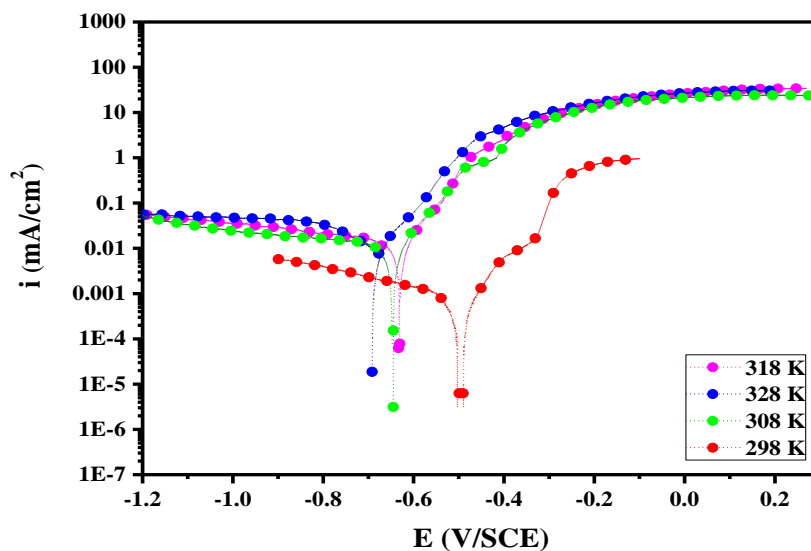


**Fig. 5:** Potentiodynamic polarization curves of tinplate in 3% NaCl (pH = 2) in the presence of 0.5 g/L of NEO at various temperatures.

However, the adsorption process was well elucidated by using a thermodynamic model. A kinetic model was another useful tool to explain the mechanism of corrosion inhibition. To calculate kinetic and thermodynamic activation parameters in the absence and presence of 0.5g/L of NEO such as activation energy  $E_a$ , entropy  $\Delta S_a$  and enthalpy  $\Delta H_a$  of activation, Arrhenius Eq. (4) [39] and its alternative formulation called transition state Eq. (5) [40] are used:

$$I_{corr} = k \exp\left(-\frac{E_a}{RT}\right) \quad (4)$$

$$I_{corr} = \frac{RT}{Nh} \exp\left(\frac{\Delta S_a}{R}\right) \exp\left(-\frac{\Delta H_a}{RT}\right) \quad (5)$$

Where R is the universal gas constant, T is the absolute temperature, h is Plank's constant, N is Avogadro's number, and A is the pre-exponential factor.

**Table 4:** Electrochemical parameters for tinplate in 3 % NaCl (pH = 2) in the absence and presence of 0.5 g/L of NEO at various temperatures.

	T(K)	$-E_{\text{corr}}$ (mV /SCE)	$i_{\text{corr}}$ ( $\mu\text{A cm}^{-2}$ )	$-\beta_c$ (mV dec $^{-1}$ )	$\eta_{\text{Tafel}}$ (%)
Blank	298	585	7700	271.3	—
	308	505	12000	115.8	—
	318	667	16600	110.7	—
	328	550	22800	95.3	—
0.5 g/L of NEO	298	489	900	102.7	88
	308	580	3500	90.0	71
	318	628	8200	87.0	50
	328	630	14400	76.0	36

The activation energy  $E_a$  is calculated from the slope of the plots of  $\text{Ln}(i_{\text{corr}})$  vs.  $1/T$  (Fig. 6). Plots of  $\text{Ln}(i_{\text{corr}}/T)$  vs.  $1/T$  give straight lines with slopes of  $\Delta H_a/R$  and intercepts of  $(\text{Ln}(R/Nh) + \Delta S_a/R)$  as shown in Fig. 7. From equation 5, the values of  $\Delta H_a$  and  $\Delta S_a$  can be calculated. The calculated parameters are collected in Table 5. It is seen that the activation energy  $E_a$  increases with the presence of NEO indicating a physical (electrostatic) mechanism of adsorption [41].

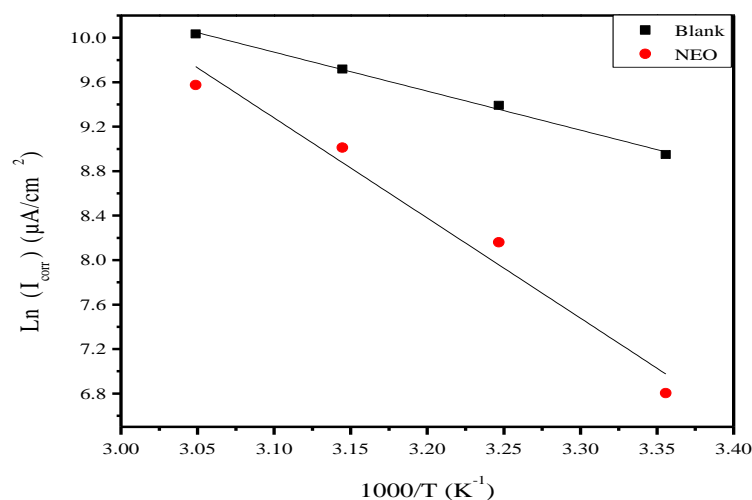


**Fig. 6:** Arrhenius plots of tinplate in 3% NaCl (pH = 2) in the absence and presence of 0.5g/L of NEO.

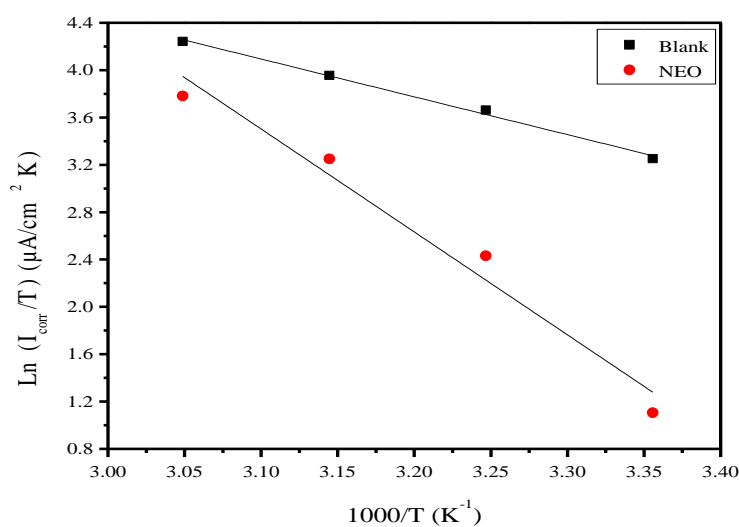


**Fig. 7:** Transition Arrhenius plots of tinplate in 3% NaCl (pH = 2) in the absence and presence of 0.5 g/L of NEO.

**Table 5:** Values of activation thermodynamic parameters for tinplate in 3% NaCl (pH=2) in the absence and presence of NEO

	$E_a$ (kJ/mol)	$\Delta H_a$ (kJ/mol)	$\Delta S_a$ (J mol <sup>-1</sup> K <sup>-1</sup> )
Blank	29.15	26.55	-81.19
0.5 g/L of NEO	74.88	72.28	55.65

It is noted also that all parameters of corrosion process increases with NEO concentration. So, the positive value of the enthalpy  $\Delta H_a$  is an endothermic nature of the tinplate dissolution process [41], while the increase of the entropy of activation  $\Delta S_a$  reveals that an increase in disordering takes place on going from reactant to the activated complex [42]. This behavior can be explained as a result of the replacement process of water molecules during adsorption of NEO on tinplate surface.

### 3.4. Adsorption Isotherm

The inhibitor action in aggressive acid media is assumed to be related to its adsorption at the metal/solution interface. This adsorption can be regarded as a substitution adsorption process between the organic molecule in the aqueous solution Org(sol) and the water molecules on the metallic surface H<sub>2</sub>O(ads) [43]:



where Org(sol) and Org(ads) are the organic molecules in the aqueous solution and adsorbed on the metallic surface, respectively, H<sub>2</sub>O(ads) is the water molecules on the metallic surface, n is the size ratio representing the number of water molecules replaced by one molecule of organic adsorbate. When the equilibrium of the process described in this equation is reached, it is possible to obtain different expressions of the adsorption isotherm plots, and thus the surface coverage degree ( $\theta$ ) can be plotted as a function of the studied inhibitor concentration [44]. The Langmuir adsorption isotherm was found to give the best description of the adsorption behaviour of NEO molecules. In this case, the surface coverage ( $\theta$ ) of the inhibitor on tinplate surface is related to its concentration in the solution according to the following equation:

$$\frac{\theta}{1-\theta} = K_{\text{ads}} C_{\text{inh}} \quad (7)$$

Rearranging this equation gives:

$$\frac{C_{\text{inh}}}{\theta} = \frac{1}{K_{\text{ads}}} + C_{\text{inh}} \quad (8)$$

where  $\theta$  is the surface coverage degree,  $C_{\text{inh}}$  is the inhibitor concentration in the electrolyte and  $K_{\text{ads}}$  is the equilibrium constant of the adsorption process where its value may be taken as a measure of the strength of the adsorption forces between the inhibitor molecules and the metal surface [45]. To calculate this parameter, the straight lines were drawn using the least squares method. The experimental (points) and calculated isotherm (lines) are plotted in Fig. 8.

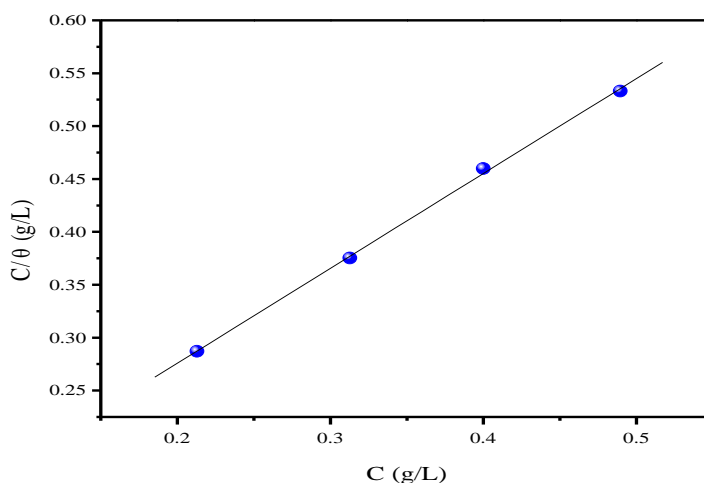
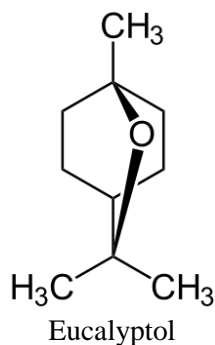


**Fig. 8:** Langmuir adsorption isotherm of NEO on tinplate surface in 3% NaCl (pH = 2) solution at 298 K.

A very good fit is observed with a regression coefficient ( $R^2$ ) up to 0.99 and the obtained line have slope very close to unity, which suggests that the experimental data is well described by Langmuir isotherm and exhibits single-layer adsorption characteristic [46].

Moreover it is not possible to discuss the adsorption behavior of plant extracts and essential oils as inhibitors in terms of thermodynamic parameters, such as the standard free energy of adsorption value because the molecular mass of the extract and oil components is not known. Sure that the Eucalyptol acts as the major component, but the intermolecular synergistic effect of various constituents of the natural oil. The same limitation has been noted by some authors [47-49].



## Conclusions

From the obtained results, we can be concluded that NEO acts as efficient corrosion inhibitor for tinplate in 3% NaCl with pH = 2 solution. It is found that the inhibition efficiency increases with inhibitor concentration to reach a maximum of 88 % at 0.5 g/L and decreases with temperature. Tafel parameters indicated that this inhibitor is mixed-type in nature at 0.5 g/L and it is cathodic type at the concentration range 0.1 g/L- 0.4 g/L. EIS experimental data revealed frequency distribution of the capacitance, simulated as constant phase element. The impedance results indicated that the polarization resistance values ( $R_p$ ) increase and double layer capacitance ( $C_{dl}$ ) decrease with the concentration of NEO. This result can be attributed to the increase of thickness of electrical double layer. The adsorption of NEO molecules on the surface of tinplate in 3 % NaCl follows a Langmuir adsorption isotherm.

## References

- Bammou L., Chebli B., Salghi R., Bazzi L., Hammouti B., Mihit M., Idrissi H., *Green Chem. Lett. Rev.* 3 (2010) 173.
- Perring L., Basic-Dvorzak M., *Anal. Bioanal. Chem.* 374 (2002) 235.
- Boogaard P.J., Boisset M., Blunden S., Davies S., Ong T.J., Taverne J-P., *Food Chem. Toxicol.* 41 (2003) 1663.
- Shimbo S., Matsuda-Inoguchi N., Watanabe T., Sakurai K., Date C., Nishimura A., Nakatsuka H., Saito H., Arisawa K., Ikeda M., *Food Addit. Contam.* 24 (2007) 535.
- Bastidas J., Cabañes J., Catalá R., *Prog. Org. Coat.* 30 (1997) 9.
- Brotons J.A., Olea-Serrano M.F., Villalobos M., Pedraza V., Olea Environ N., *Health Perspect.* 103 (1995) 608.
- Catala R., Cabanes J., Bastidas J., *Corros. Sci.* 40 (1998) 1455.
- Cottier S., Feigenbaum A., Mortreuil P., Reynier A., Dole P., Riquet A., Agric J., *Food Chem.* 46 (1998) 5254.
- Bentiss F., Traisnel M., Lagrenee M., *Corros. Sci.* 42 (2000) 127.
- Morad M.S.S., Herma A.A.A.S., *J. Chem. Technol. Biotechnol.* 76 (2001) 401.
- Ghazoui A., Saddik R., Benchat N., Hammouti B., Guenbour M., Zarrouk A., Ramdani M., *Der Pharm. Chem.* 4(1) (2012) 352.
- Zarrok H., Saddik R., Oudda H., Hammouti B., El Midaoui A., Zarrouk A., Benchat N., Ebn Touhami M., *Der Pharm. Chem.* 3(5) (2011), 272.
- Zarrouk A., Hammouti B., Touzani R., Al-Deyab S.S., Zertoubi M., Dafali A., Elkadiri S., *Int. J. Electrochem. Sci.* 6 (10) (2011) 4939.
- Zarrouk A., Hammouti B., Dafali A., Zarrok H., *Der Pharm. Chem.* 3(4) (2011) 266.
- Ghazoui A., Zarrouk A., Benchat N., Salghi R., Assouag M., El Hezzat M., Guenbour A., Hammouti B., *Chem J. Pharm. Res.* 6(2) (2014) 704.
- Zarrok H., Zarrouk A., Salghi R., Oudda H., Hammouti B., Assouag M., Taleb M., Ebn Touhami M., Bouachrine M., Boukhris S., *Chem J. Pharm. Res.* 4(12)(2012) 5056.

17. Zarrok H., Zarrouk A., Salghi R., Assouag M., Hammouti B., Oudda H., Boukhris S., Al Deyab S.S., Warad I., *Der Pharm. Lett.* 5(2) (2013) 43.
18. Belayachi M., Serrar H., Zarrok H., El Assyry A., Zarrouk A., Oudda H., Boukhris S., Hammouti B., Ebenso E.E., Geunbour A., *Int. J. Electrochem. Sci.* 10(4) (2015) 3010.
19. Zarrouk A., Zarrok H., Salghi R., Tourir R., Hammouti B., Benchat N., Afrine L.L. , Hannache H., El Hezzat M., Bouachrine M., *Chem J. Pharm. Res.* 5(12) (2013) 1482.
20. Zarrok H., Zarrouk A., Salghi R., Ebn Touhami M., Oudda H., Hammouti B., Tourir R., F. Bentiss F., Al-Deyab S.S., *Int. J. Electrochem. Sci.* 8(4) (2013) 6014.
21. Ben Hmamou D., Aouad M.R., Salghi R., Zarrouk A., Assouag M., Benali O., Messali M., Zarrok H., Hammouti B., *Chem J. Pharm. Res.* 4(7) (2012) 34984.
22. Eddy N.O, Ebenso E.E., *African J. Pure Appl. Chem.* 2(6) (2008) 1.
23. Chetouani A., Hammouti B., Benkaddour M., *Pigm. Resin.Technol.* 33 (2004) 26.
24. Chaieb E.L., Bouyanzer A., Hammouti B., Benkaddour M., Berrabah M., *Trans SAEST* 39 (2004) 58
25. Bendahou M., Benabdellah M., Hammouti B., *PigmResinTechnol.* 35 (2006) 95.
26. Bouyanzer A., Hammouti B., *PigmResinTechnol.* 33(2004) 287
27. Benabdellah M., Bendahou M., Hammouti B., Benkaddour M., *Appl Surf Sci.*8 (2005) 30
28. Lotfi N., Benhiba F., Chahboun N., Bourazmi H., El Hezzat M., Al Hamzi A. H., Zarrok H., Guenbour A., Ouhsine M., Oudda H. and Zarrouk A., *Der Pharm. Lett.* 7 (9) (2015) 1.
29. Gong M., Mao F., Wu J., Zeng X., *Corros Prot-NANCHANG-27* (2006) 576.
30. Bouyanzer A., Majidi L., Hammouti B., *Bull Electrochem.* 22 (2006) 321.
31. Bouyanzer A., Hammouti B., Majidi L., *Mater. Letters* 60 (2006) 2840.
32. Bouyanzer A., Majidi L., Hammouti B., *Bull. Elect.* 22(2006) 321.
33. Dehri I., Ozcan M., *Mater. Chem. Phys.* 98 (2006) 316.
34. Ritchie I.M., Bailey S., Woods R., *Adv. Colloid Interface Sci.*80 (1999) 183.
35. Jeyaprabha C., Sathhiyanarayanan S., Venkatachari G., *Electrochim. Acta* 51 (2006) 4080.
36. Ozcan M., Dehri I., *Prog. Org. Coat.*51 (2004) 181.
37. Erbil M., *Chimica Acta Turcica* .1 (1988) 59.
38. Lagrenee M., Mernari B., Bouanis M., Traisnel M., Bentiss F., *Corros. Sci.* 44 (2002) 573.
39. Lgaz H., Saadouni M., Salghi R., Jodeh S., Ramli Y., Souizi A., Oudda H., *Der Pharm. Lett.* 8 (2016) 167.
40. Lgaz H., ELaoufir Y., Ramli Y., Larouj M., Zarrok H., Salghi R., Zarrouk A., Elmidaoui A., Guenbour A., Essassi El M., Oudda H., *Der Pharm. Chem.*7 (2015) 36.
41. Verma C., Quraishi M.A., Singh A., *J. Mol. Liq.* 212 (2015) 804.
42. Lgaz H., Saadouni M., Salghi R., Jodeh S., Ramli Y., Souizi A., Oudda H., *Der Pharm. Lett.* 8(2016) 167.
43. Behpour M., Ghoreishi S.M., Gandomi-Niasar A., Soltani N., Salavati-Niasari M., *J. Mater. Sci.* 44 (2009) 2444.
44. Labjar N., Bentiss F., Lebrini M., Jama C., El hajjaji S., *Inter. J. Corros.* (2011), Article ID 548528.
45. Amin M.A., *J. Appl. Electrochem* .36 (2006) 215.
46. Ebenso E.E., I.B. Obot I.B., *Int. J. Electrochem. Sci.* 5 (2010) 2012.
47. Kanojia R., Singh G., *Surf. Eng.* 21 (2005) 180.
48. Bouoidina A., El-Hajjaji F., Chaouch M., Abdellaoui A., Elmsellem H., Rais Z., Filali Baba M., Lahkimi A., Hammouti B. and Taleb M., *Der Pharma Chemica*, 8(13) (2016)149-157
49. Bammou L., Mihit M., Salghi R., Bazzi L., Bouyanzer A., Al-Deyab S.S., Hammouti B., *Int. J. Electrochem. Sci.*, 6 N°5 (2011) 1454-1467.

(2017) ; <http://www.jmaterenvironsci.com>